# Analysis of Inhomogeneously Dielectric Filled Cavities Coupled to Dielectric-Loaded Waveguides: Application to the Study of NRD-Guide Components

Juan A. Monsoriu, Benito Gimeno, *Member, IEEE*, Enrique Silvestre, and Miguel V. Andrés, *Member, IEEE*

***Abstract*—In this paper, we present two contributions. First, we develop a computationally efficient technique for the full-wave characterization of inhomogeneously dielectric-filled cavities connected to inhomogeneously dielectric-loaded waveguides. This method is based on the expansion of the electromagnetic field within the cavity in terms of their solenoidal and irrotational modes. The presented formulation allows the treatment of hybrid modes in the waveguide ports, where the definition of a characteristic modal impedance or admittance is not possible. The multimode scattering matrix of the structure is computed throughout an efficient implementation of the orthonormal-basis method for the calculation of the cavity modes. Secondly, we have employed the present technique for the analysis and design of nonradiative dielectric (NRD) guide components and discontinuities. Moreover, the application of the bi-orthonormal-basis method for the calculation of the full-spectrum of NRD guides is demonstrated as being a very efficient approach for the rigorous treatment of such guides. Next, an efficient computer-aided design tool has been developed for the analysis of complex NRD-guide circuits. We have compared our simulations with theoretical and experimental results available in the technical literature, fully validating our software. This code has been employed for the specific analysis of a linear continuous taper to match two NRD guides with different widths, demonstrating a considerable reduction of the return losses over a wide frequency band. Finally, stopband and bandpass NRD-guide filters based on an electromagnetic-bandgap concept are presented.**

***Index Terms*—Bi-orthonormality relationship, electromagnetic bandgap (EBG), dielectric-loaded cavity, Galerkin method, nonradiative dielectric (NRD) guide, orthonormality relationship.**

## I. Introduction

In MANY applications of electromagnetic-field theory, the rigorous analysis of microwave cavities is a crucial point. The study of the junction between a central cavity to the adjacent connected waveguides has been analyzed over the last years by several authors [1]–[5]. In particular, the boundary-integral–resonant-mode expansion (BI–RME) technique [6] has been efficiently applied to the analysis of cavities with arbitrary geometry involving metallic obstacles [7], [8]. The analyzed structures in the referred studies did not include the presence of dielectric inhomogeneities. However, the study of dielectric-loaded cavities has deserved the attention of numerous research groups over the last decades mainly due to the applications of dielectric resonators as microwave filters in satellite and mobile telecommunications because of their small size, low loss, and temperature stability. Thus, a large number of papers are found in the technical literature dedicated to the numerical calculations of the eigenmodes and eigenvectors of canonical metallic cavities loaded with dielectric resonators [9]–[17]. In the same way, the study in detail of the problem of the junction between a dielectric-loaded cavity and their input and output waveguide ports attracts the attention of numerous researchers due to the applications of such subsystems in microwave dielectric-resonator filters. Several techniques such as the mode matching [18], [19], finite-element method (FEM) [20], [21], and finite-difference time-domain (FDTD) procedure [22] have been employed to deal with this problem.

Within this demanding scenario, the numerical modeling of dielectric-loaded cavities connected to inhomogeneously dielectric-filled waveguides is the main objective of this paper. Inspired by the aforementioned BI–RME method, we have developed a rigorous and computationally efficient technique based on the expansion of the electromagnetic field with respect to the complete set of modes of the closed cavity. Substituting these expansions into the Maxwell's equations in the presence of virtual driving currents—following the standard procedure proposed in [23] and [24]—the expansion coefficients of the electromagnetic field inside the cavity are expressed in terms of the waveguide fields since these assumed currents are, in their turn, induced by the total fields in the waveguides at the cavity ports. In this way, the expansion coefficients of the cavity modes can be eliminated, obtaining a linear system of equations relating the modal coefficients of the waveguide modes, which allows to lead directly to the computation of the multimode scattering matrix.

On the other hand, in order to produce a versatile algorithm valid for the analysis of complex structures, we have considered

Manuscript received September 2, 2003; revised January 19, 2004. This work was supported by the Ministerio de Ciencia y Tecnología, Spanish Government under Research Project TIC2000-0591-C03 and Research Project TIC2002-04 527-C02-02.

J. A. Monsoriu is with the Departamento de Física Aplicada, Universidad Politécnica de Valencia, E-46022 Valencia, Spain.

B. Gimeno and M. V. Andrés are with the Departamento de Física Aplicada and the Institut de Ciència dels Materials, Universidad de Valencia, E-46100 Burjassot (Valencia), Spain.

E. Silvestre is with the Departamento de Óptica, Universidad de Valencia, E-46100 Burjassot (Valencia), Spain.

Digital Object Identifier 10.1109/TMTT.2004.830484

dielectric-loaded guides as input and output waveguide ports. As it is well known, the modal spectrum supported by dielectric-loaded waveguides consists of TE, TM, and hybrid modes [24]. In the case of the TE and TM modes, it is possible to define—at least formally—a characteristic modal impedance. For instance, the characteristic modal impedances of a rectangular dielectric slab loaded rectangular waveguide are given by (see [24, Ch. 6])

$$Z^{\mathrm{TE}^x_{r,s}} = \frac{k^2 - (r\pi/a)^2}{\omega\varepsilon\beta_{r,s}} \quad Z^{\mathrm{TM}^x_{r,s}} = \frac{\omega\mu\beta_{r,s}}{k^2 - (r\pi/a)^2} \tag{1}$$

for the $\mathrm{TE}^x$ and $\mathrm{TM}^x$ modes (also denoted as longitudinal section electric (LSE) and longitudinal section magnetic (LSM), respectively). It can be observed in these expressions that the modal impedance of the $\mathrm{TM}^x$ modes is completely well defined, whereas the corresponding one to the modes $\mathrm{TE}^x$ depends on the point since the dielectric permittivity is spatially dependent. In this sense, the $\mathrm{TE}^x$ modal impedance is a function of the position. Consequently, the standard mode-matching techniques based on the definition of characteristic modal impedances or admittances [2]–[4], [6]–[8], [18] cannot be directly applied when inhomogeneous dielectric waveguides are involved. Moreover, for the general case of hybrid modes, the definition of a modal characteristic impedance or admittance is not always possible (see, for instance, the image dielectric guide [25]). The merit of the current method is to provide an efficient and rigorous algorithm suitable for the treatment of the hybrid modes present in dielectric-loaded guides.

As a practical application, we have used our technique for the analysis of integrated nonradiative dielectric (NRD) components. The NRD guide is recognized as the first dielectric waveguide that has been found practically meaningful in the low-cost circuit design for millimeter and sub-millimeter bands; over the last decades, numerous publications can be found in the scientific literature for the analysis and design of NRD integrated circuits (see, e.g., [26]–[30]). Modeling and characterization of NRD-guide components is an important task for the correct design and optimization of complex circuits based on NRD guides. To this end, we have employed the orthonormal-basis technique [17] for the calculations of the eigenmodes and eigenvectors of the dielectric-loaded cavities. Moreover, the bi-orthonormal-basis method [31], [32] has been successfully used for the evaluation of the full-modal spectrum of the NRD waveguides. Finally, we analyze several stop-band and bandpass NRD filters based on the electromagnetic bandgap (EBG) concept.

This paper is organized as follows. In Section II, we present theoretical formalism. In Section III, we compare our results with those theoretical and experimental presented by other authors to fully validate the theory. Next, we tackle the analysis of a novel transition between two NRD guides and the study of EBG filters in NRD technology. Finally, we summarize our conclusions in Section IV.

## II. Theory

Let us consider an inhomogeneously dielectric filled cavity of arbitrary shape and perfectly conducting boundaries, as shown in Fig. 1, where $\mathbf{n}$ is the unit vector directed outwards normal to the wall surface of the cavity. The dielectric filling medium is assumed to be lossless ($\varepsilon_r = \varepsilon_r(\mathbf{r})$ is a real function) and nonmagnetic ($\mu_r = 1$). The cavity presented in Fig. 1 is connected to $N$ inhomogeneously dielectric filled waveguides of uniform transverse cross section. As it is well known, the full set of modes supported by these guides involve, in the most general case, hybrid modes. Thus, the developed theory presented in this paper is not only restricted to the conventional TE and TM modes (or LSE and LSM modes), also being applicable to the most general case of hybrid modes. We assume that the time dependence is always implicit and has a harmonic form $e^{j\omega t}$.

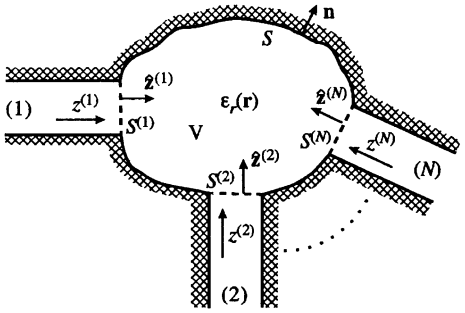


Fig. 1. Inhomogeneously dielectric-filled cavity connected to $N$ dielectric-loaded waveguide ports.

### A. Eigenmode Expansion in an Inhomogeneously Dielectric Filled Closed Cavity With Sources

The electric and magnetic fields inside a closed cavity containing inhomogeneous dielectric media can be expanded in terms of two kinds of modes, i.e., the solenoidal and irrotational modes [23], [24], [33]. The differential equations governing the solenoidal magnetic and electric modes $\mathbf{h}_n$ and $\mathbf{e}_n$, respectively, are given by

$$\nabla \times \frac{1}{\varepsilon_r} \nabla \times \mathbf{h}_n = k_n^2 \mathbf{h}_n \text{ and } \nabla \cdot \mathbf{h}_n = 0 \tag{2}$$

and

$$\nabla \times \nabla \times \mathbf{e}_n = k_n^2 \varepsilon_r \mathbf{e}_n \text{ and } \nabla \cdot \varepsilon_r \mathbf{e}_n = 0 \tag{3}$$

where $k_n^2 = \omega_n^2 \varepsilon_0 \mu_0$ is the corresponding eigenvalue, whereas the irrotational magnetic and electric modes $\mathbf{g}_n$ and $\mathbf{f}_n$, respectively, are described by the following eigenvalue problems:

$$\nabla\nabla \cdot \mathbf{g}_n = -p_n^2 \mathbf{g}_n \text{ and } \nabla \times \mathbf{g}_n = 0 \tag{4}$$

and

$$\nabla\nabla \cdot \varepsilon_r \mathbf{f}_n = -l_n^2 \mathbf{f}_n \text{ and } \nabla \times \mathbf{f}_n = 0 \tag{5}$$

where $p_n^2$ and $l_n^2$ are their corresponding eigenvalues [24]. The fields in (2)–(5) have to fulfill the proper boundary conditions on the surface $S$ as follows:

$$\begin{aligned} \mathbf{n} \cdot \mathbf{h}_n &= 0 \\ \mathbf{n} \times \mathbf{e}_n &= 0 \\ \mathbf{n} \cdot \mathbf{g}_n &= 0 \\ \mathbf{n} \times \mathbf{f}_n &= 0. \end{aligned} \tag{6}$$

These modes satisfy the following orthonormality relationships:

$$\begin{aligned}\langle \mathbf{h}_m, \mathbf{h}_n \rangle &= \langle \mathbf{g}_m, \mathbf{g}_n \rangle = \delta_{m,n} \\ \langle \mathbf{h}_m, \mathbf{g}_n \rangle &= 0 \\ \langle \mathbf{e}_m, \varepsilon_r \mathbf{e}_n \rangle &= \langle \mathbf{f}_m, \varepsilon_r \mathbf{f}_n \rangle = \delta_{m,n} \\ \langle \mathbf{e}_m, \varepsilon_r \mathbf{f}_n \rangle &= 0 \end{aligned} \tag{7}$$

where $\langle \mathbf{v}, \mathbf{w} \rangle = \int_V \mathbf{v} \cdot \mathbf{w} dV$ is the standard inner product for real fields in the cavity $V$ and $\delta_{m,n}$ is the Kronecker delta. Furthermore, each solenoidal eigenfunction can be selected so as to make a pair $\mathbf{h}_n$ and $\mathbf{e}_n$ satisfying

$$\begin{aligned}\nabla \times \mathbf{h}_n &= k_n \varepsilon_r \mathbf{e}_n \\ \nabla \times \mathbf{e}_n &= k_n \mathbf{h}_n. \end{aligned} \tag{8}$$

Thus, by using (7), the electromagnetic field inside the cavity can be expanded in terms of the cavity modes

$$\mathbf{E} = \sum_n E_n \mathbf{e}_n + \sum_n F_n \mathbf{f}_n \tag{9a}$$

$$\mathbf{H} = \sum_n H_n \mathbf{h}_n + \sum_n G_n \mathbf{g}_n \tag{9b}$$

where $E_n, F_n, H_n$, and $G_n$ are the modal expansions coefficients given by

$$\begin{aligned} H_n &= \langle \mathbf{H}, \mathbf{h}_n \rangle \\ E_n &= \langle \mathbf{E}, \varepsilon_r \mathbf{e}_n \rangle \\ G_n &= \langle \mathbf{H}, \mathbf{g}_n \rangle \\ F_n &= \langle \mathbf{E}, \varepsilon_r \mathbf{f}_n \rangle. \end{aligned} \tag{10}$$

To proceed, we write Maxwell's equations in the presence of electric and magnetic current density distributions $\mathbf{J}_e$ and $\mathbf{J}_m$, respectively, as follows:

$$\begin{aligned}\nabla \times \mathbf{E} &= -j\omega\mu_0 \mathbf{H} - \mathbf{J}_m \\ \nabla \times \mathbf{H} &= j\omega\varepsilon_0 \varepsilon_r \mathbf{E} + \mathbf{J}_e. \end{aligned} \tag{11}$$

Those current densities play the role of driving currents, capable of supplying power to the cavity [33]. In our problem, they are fictitious surface currents restricted to the $N$ connecting port surfaces, $S^{(\nu)}$ (see Fig. 1), given by the tangential electric and magnetic components over the waveguide port surface $\mathbf{J}_m = \mathbf{n} \times \mathbf{E}_T$ and $\mathbf{J}_e = -\mathbf{n} \times \mathbf{H}_T$, respectively, as will be expounded upon in Section II-B.

By expanding the $\mathbf{H}$-like function $\nabla \times \mathbf{E}$ in terms of both types of magnetic modes, and the $\mathbf{E}$-like function $\varepsilon_r^{-1} \nabla \times \mathbf{H}$ in terms of the electric ones [24], and after some algebraic manipulations, we obtain the expansion coefficients in terms of the equivalent magnetic current density

$$\begin{aligned} E_n &= \sum_{\nu=1}^{N} \frac{k_n}{k_0^2 - k_n^2} \int_{S^{(\nu)}} (\mathbf{n} \times \mathbf{E}_T) \cdot \mathbf{h}_n \, dS \\ F_n &= 0 \\ H_n &= \frac{j\omega\varepsilon_0}{k_n} E_n \\ G_n &= \sum_{\nu=1}^{N} \frac{j}{\omega\mu_0} \int_{S^{(\nu)}} (\mathbf{n} \times \mathbf{E}_T) \cdot \mathbf{g}_n \, dS \end{aligned} \tag{12}$$

where $k_0 = \omega\sqrt{\varepsilon_0 \mu_0}$ is the wavenumber of the free space.

### *B. Scattering Matrix of an Inhomogeneously Dielectric Filled Cavity*

The objective here is to obtain an alternative procedure, always based on the theory of cavities, as described in detail in Section II-A, to develop a multimode scattering matrix for the arbitrary cavity depicted in Fig. 1, connected to $N$ ports.

To set up the formulation, we define the following inner products for the fields in the waveguide ports connected to the cavity

$$\langle \mathbf{v}, \mathbf{w} \rangle^{(\nu)} \equiv \int_{S^{(\nu)}} (\mathbf{v} \times \mathbf{w}) \cdot \hat{\mathbf{z}}^{(\nu)} \, dS \tag{13}$$

where $\mathbf{v}$ and $\mathbf{w}$ are arbitrary complex vectors defined on the transverse cross section of the $\nu$th waveguide, and $\hat{\mathbf{z}}^{(\nu)}$ is the unitary vector normal to the cross section of each uniform guide, directed inside the cavity (see Fig. 1). These inner products are obviously based on the well-known orthonormality relationship of the electromagnetic field in a waveguide (see, e.g., [24]) in such a manner that

$$\left\langle \mathbf{e}_p^{(\nu)}, \mathbf{h}_q^{(\nu)} \right\rangle^{(\nu)} = \delta_{p,q} \tag{14}$$

where $\mathbf{e}_p^{(\nu)}$ and $\mathbf{h}_q^{(\nu)}$ are the normalized transverse electric and magnetic modal vectors of the $\nu$th waveguide. Thus, the transverse electric and magnetic fields in the waveguide can be expressed as series of the normalized modal vectors.

In order to calculate the multimode scattering matrix of the structure, let us consider that some modes of certain guides are incident on their corresponding cavity ports with nonzero amplitudes $a_q^{(\nu)+}$. Consequently, the electromagnetic field will be excited in the cavity, and a substantial amount of power will leak out to the other ports with amplitudes $a_q^{(\nu)-}$. Thus, considering that the reference planes of all guides coincide with their corresponding cavity ports ($z^{(\nu)} = 0$), the tangential field in the connecting waveguide ports ($\nu = 1, 2, \ldots, N$) can be expressed as follows:

$$\mathbf{E}_T^{(\nu)} = \sum_{q=1}^{Q(\nu)} b_q^{(\nu)} \mathbf{e}_q^{(\nu)} \tag{15a}$$

$$\mathbf{H}_T^{(\nu)} = \sum_{q=1}^{Q(\nu)} c_q^{(\nu)} \mathbf{h}_q^{(\nu)} \tag{15b}$$

where $Q(\nu)$ is the number of modes considered (both propagative and evanescent) in the $\nu$th port, and $b_q^{(\nu)}$ and $c_q^{(\nu)}$ are coefficients given, in terms of the incoming and outgoing amplitudes, by

$$b_q^{(\nu)} = a_q^{(\nu)+} + a_q^{(\nu)-} \quad c_q^{(\nu)} = a_q^{(\nu)+} - a_q^{(\nu)-}. \tag{16}$$

To continue, we introduce the total tangential electric field at the connecting ports (15a) into the cavity modal expansion coefficients (12), just obtaining the following expressions:

$$\begin{aligned} E_n &= \sum_{\nu=1}^{N} \frac{k_n}{k_0^2 - k_n^2} \sum_{q=1}^{Q(\nu)} b_q^{(\nu)} \alpha_{n,q}^{(\nu)} \\ F_n &= 0 \\ H_n &= \frac{j\omega\varepsilon_0}{k_n} E_n \\ G_n &= \sum_{\nu=1}^{N} \frac{j}{\omega\mu_0} \sum_{q=1}^{Q(\nu)} b_q^{(\nu)} \sigma_{n,q}^{(\nu)} \end{aligned} \tag{17}$$

where $\alpha_{n,q}^{(\nu)}$ and $\sigma_{n,q}^{(\nu)}$ represent the coupling coefficients between the cavity modes and guided modes of the ports

$$\alpha_{n,q}^{(\nu)} \equiv -\left\langle \mathbf{e}_q^{(\nu)}, \mathbf{h}_n \right\rangle^{(\nu)}$$
$$\sigma_{n,q}^{(\nu)} \equiv -\left\langle \mathbf{e}_q^{(\nu)}, \mathbf{g}_n \right\rangle^{(\nu)}. \tag{18}$$

To conclude the formulation, we apply the boundary condition of the magnetic field on the apertures

$$\mathbf{H}|_{S^{(\nu)}} = \mathbf{H}_T^{(\nu)}. \tag{19}$$

By inserting into this expression (9b) and (15b), we obtain the following set of equations:

$$\sum_n H_n \mathbf{h}_n|_{S^{(\nu)}} + \sum_n G_n \mathbf{g}_n|_{S^{(\nu)}} = \sum_{q=1}^{Q(\nu)} c_q^{(\nu)} \mathbf{h}_q^{(\nu)} \tag{20}$$

which can be exploited by applying the Galerkin's procedure, just integrating in the surface of each waveguide port, and where $\nu$ range all the waveguides $(1, \ldots, N)$

$$\left\langle \mathbf{e}_p^{(\nu)}, \sum_n H_n \mathbf{h}_n + \sum_n G_n \mathbf{g}_n \right\rangle^{(\nu)} = \left\langle \mathbf{e}_p^{(\nu)}, \sum_q c_q^{(\nu)} \mathbf{h}_q^{(\nu)} \right\rangle^{(\nu)}. \tag{21}$$

Making use of the orthonormality property of the waveguide modes (14), the second term of (21) is directly evaluated, being equal to the modal coefficient $c_p^{(\nu)}$, whereas the first term can be developed by means of the coefficients given in (17), just transforming our problem into a set of linear equations as

$$\sum_{\mu=1}^{N} \sum_{q=1}^{Q(\mu)} P_{p,q}^{(\nu,\mu)} b_q^{(\mu)} = c_p^{(\nu)} \tag{22}$$

where the elements of the matrix $P_{p,q}^{(\nu,\mu)}$ turn out to be defined as

$$P_{p,q}^{(\nu,\mu)} \equiv \sum_n \frac{-j\omega\varepsilon_0}{k_0^2 - k_n^2} \alpha_{n,p}^{(\nu)} \alpha_{n,q}^{(\mu)} + \frac{-j}{\omega\mu_0} \sum_n \sigma_{n,p}^{(\nu)} \sigma_{n,q}^{(\mu)}. \tag{23}$$

Equation (22) can be rewritten in matrix form as

$$\begin{pmatrix} P^{(1,1)} & P^{(1,2)} & \ldots & P^{(1,N)} \\ P^{(2,1)} & P^{(2,2)} & \ldots & P^{(2,N)} \\ \ldots & \ldots & \ddots & \ldots \\ P^{(N,1)} & P^{(N,2)} & \ldots & P^{(N,N)} \end{pmatrix} \begin{pmatrix} b^{(1)} \\ b^{(2)} \\ \vdots \\ b^{(N)} \end{pmatrix} = \begin{pmatrix} c^{(1)} \\ c^{(2)} \\ \vdots \\ c^{(N)} \end{pmatrix}$$

where each $P^{(\nu,\mu)}$ represents a submatrix containing the elements defined in (23), and $b^{(\nu)}$ and $c^{(\nu)}$ are vectors composed by the modal coefficients given in (16), all of them for fixed values of $\mu$ and $\nu$. It is worthwhile to mention that the order of this linear system is $Q_T = Q(1) + Q(2) + \cdots + Q(N)$. Finally, in order to obtain the multimode scattering matrix of the junction, the previous linear system is transformed into

$$(P + I)(a^+ + a^-) = 2a^+ \tag{24}$$

where $I$ is the unitary matrix of order $Q_T$, $P$ is the matrix containing the submatrices $P^{(\nu,\mu)}$, and $a^+$ and $a^-$ represent column vectors containing the corresponding coefficients defined in (16). The numerical solution of (24) automatically leads to the computation of the scattering matrix elements of the cavity junction.

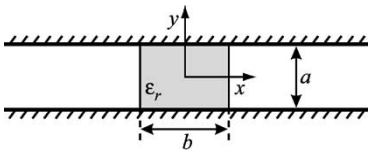


Fig. 2. Transversal cross-sectional view of a conventional NRD guide. The spacing between the two metallic plates is $a$, the dielectric thickness is $b$, and the relative dielectric permittivity is $\varepsilon_r$.

## III. Numerical Results

### A. Full Modal Analysis of NRD Guides by Means of the Bi-Orthogonal-Basis Method

In order to calculate the modes of the NRD guides (see Fig. 2), the bi-orthogonal-basis method has been employed [31]. This novel technique has been demonstrated to be computationally efficient in obtaining the full modal spectrum of dielectric-loaded guides with canonical geometries [32]. For simulation purposes, two equidistant perfect electric walls parallel to the $Y$-axis are placed far enough from the dielectric central block. This technique uses the modes of an auxiliary system to expand the modes of the problem. In our case, the auxiliary system is the homogeneous waveguide that one obtains when there is no dielectric. First, in Fig. 3, we show the modal distribution of the two first modes $\mathrm{LSM}_{1,0}$ and $\mathrm{LSE}_{1,0}$ of a conventional NRD guide. To validate the procedure developed here, a comparison of the dispersion curve of the fundamental mode between our calculations and the analytical ones obtained with the multimodal transverse resonance technique [30] is shown in Fig. 4, finding a very good agreement. For such calculation, 200 auxiliary modes have been used to expand each NRD-guide mode. The CPU time has been approximately 0.6 s per frequency point in a Pentium III at 1000 MHz.

The current method allows to consider the presence of lossy dielectric materials in a rigorous form [34] instead of employing a conventional perturbative approach. Thus, in Fig. 5, we plot the ratio between the transmission losses for the $\mathrm{LSM}_{1,0}$ mode of a conventional NRD guide calculated with our method and the values given by Dallaire and Wu in [29], which have been obtained using a perturbative method, as a function of the loss tangent. In Fig. 5, the perturbative solution would be represented by the dashed horizontal line (ratio equal to 0 dB/m). For low values of $\tan\delta$, the perturbative solution approaches monotonously to our rigorous solution, thus showing the validity region of the perturbative approach commonly employed for the calculation of the attenuation constant associated with the dielectric losses.

### B. Analysis of Discontinuities Between NRD Guides

Next, an aligned air-gap discontinuity between two identical NRD guides has been analyzed by means of the algorithm described in Section II [see Fig. 6(a)]. In this example, an empty rectangular cavity connected to two NRD guides has allowed the system to be simulated. For this simple case, the analytically obtained cavity modes of an empty rectangular metallic box (e.g., [24]) has been employed for the electromagnetic-field expansion within the cavity [see (9a) and (9b)]. In Fig. 6(b) and

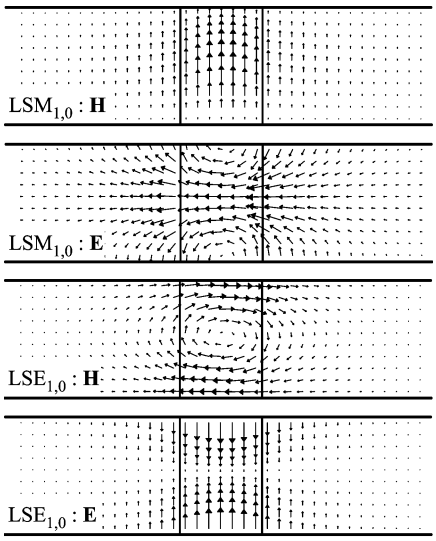


Fig. 3. Transverse electric- and magnetic-field patterns of $\mathrm{LSM}_{1,0}$ and $\mathrm{LSE}_{1,0}$ modes of a conventional NRD guide at a frequency of 28 GHz ($a = 5$ mm, $b = 3.556$ mm, $\varepsilon_r = 2.56$).

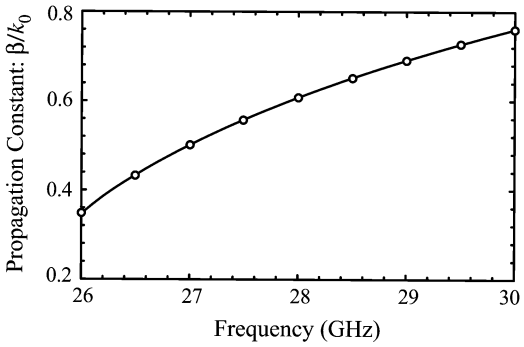


Fig. 4. Normalized propagation constant of the $\mathrm{LSM}_{1,0}$ mode of a conventional NRD guide (solid line) in comparison with the analytical results presented in [30] (plotted points) ($a = 5$ mm, $b = 3.556$ mm, $\varepsilon_r = 2.56$).

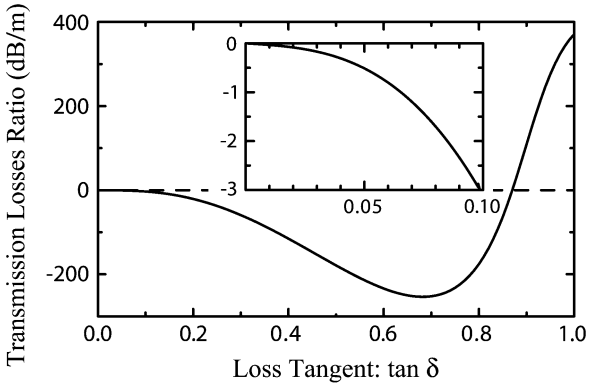


Fig. 5. Transmission-loss ratio between our simulations and the results presented in [29] for the $\mathrm{LSM}_{1,0}$ mode of a conventional NRD guide at a frequency of 28 GHz as a function of the loss tangent ($a = 5$ mm, $b = 3.556$ mm, $\varepsilon_r = 2.56$). The inset shows a detail around the origin.

(c), the reflection and transmission coefficients under $\mathrm{LSM}_{1,0}$ mode excitation are plotted together with the theoretical results presented in [30], finding a very good agreement. Note that the $\mathrm{LSE}_{1,1}$ mode is evanescent below 28.688 GHz. The intermode coupling between LSM and LSE modes has been taken into account in all simulations.

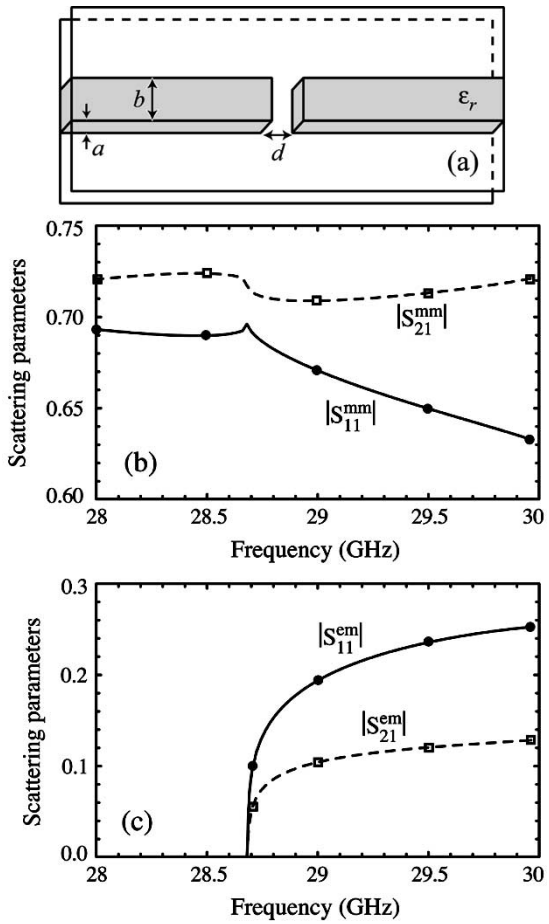


Fig. 6. Analysis of an air-gap discontinuity between two identical NRD guides ($a = 5$ mm, $b = 3.556$ mm, $\varepsilon_r = 2.56$, $d = 0.5b$). Comparison between our results (solid line) and those presented in [30] (plotted points). (a) Scheme of the structure. (b) Reflection and transmission coefficients of the $\mathrm{LSM}_{1,0}$ mode under $\mathrm{LSM}_{1,0}$ incidence. (c) Reflection and transmission coefficients of the $\mathrm{LSE}_{1,1}$ mode under $\mathrm{LSM}_{1,0}$ incidence.

The following example is devoted to the performance of an air-gap discontinuity between two NRD guides with different widths showed in Fig. 7(a). The modeling of this structure is similar to the previous one. The scattering parameters under $\mathrm{LSM}_{1,0}$ incident mode are displayed in Fig. 7(b) and (c), demonstrating the appearance of the intermode coupling between the propagative modes above 28.688 GHz. It is worthwhile to mention the significant loss of transmitted power appreciated for the case $d = 0.5b_1$ [see Fig. 7(b)] with respect to the case when the air gap disappears, i.e., $d = 0$ [see Fig. 7(c)]. This phenomenon is a physical consequence of the existing air-gap discontinuity between the NRG guides in connection with the appreciable difference of the widths.

In order to reduce this loss of transmitted power, we propose to match both guides by means of a simple linear continuous taper. This novel matching structure, which consists of the direct junction of both NRD guides through a trapezoidal dielectric central block with the same dielectric permittivity than the input and output waveguides, is showed in Fig. 8(a). To model this structure, the cavity formed by a dielectric trapezoid immersed into an empty cavity has been employed. It is worth pointing out here that our technique avoids the use of the staircase approximation, commonly used for the analysis of irregular shapes

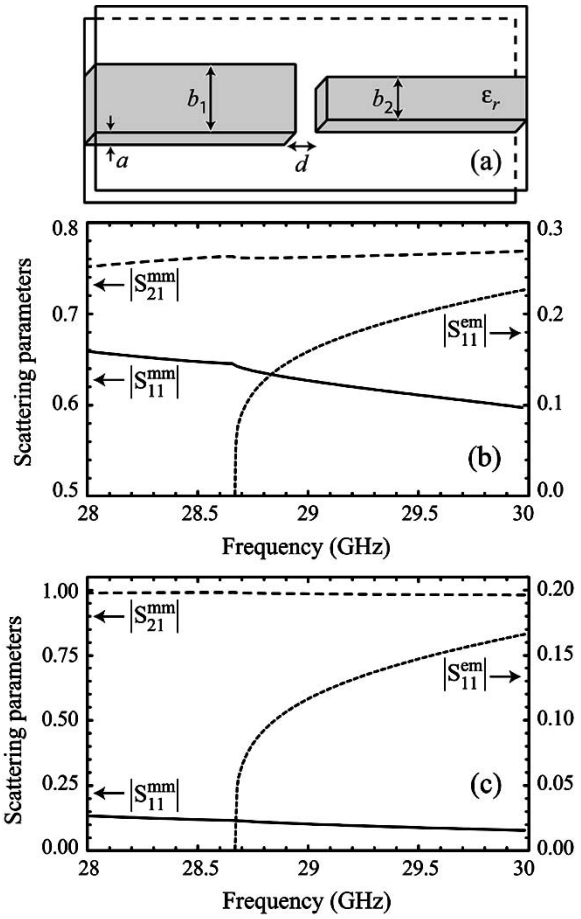


Fig. 7. Analysis of an air-gap discontinuity between two NRD guides with different widths ($a = 5$ mm, $b_1 = 5$ mm, $b_2 = 3.556$ mm, $\varepsilon_r = 2.56$). (a) Configuration of the structure. Reflection and transmission coefficients of the $\mathrm{LSM}_{1,0}$ and $\mathrm{LSE}_{1,1}$ modes under $\mathrm{LSM}_{1,0}$ incidence for (b) $d = 0.5b_1$ and (c) $d = 0$.

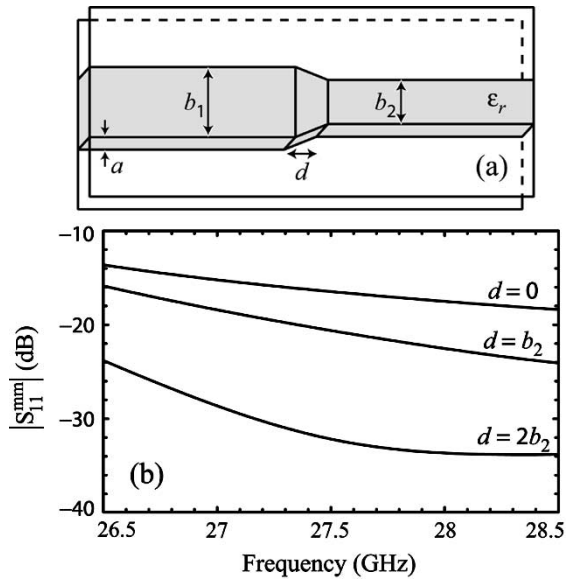


Fig. 8. Analysis of a linear continuous taper between two NRD guides with different widths ($a = 5$ mm, $b_1 = 5$ mm, $b_2 = 3.556$ mm, $\varepsilon_r = 2.56$). (a) Configuration of the structure. (b) Reflection coefficient of the $\mathrm{LSM}_{1,0}$ mode under $\mathrm{LSM}_{1,0}$ excitation for $d = 0$, $d = b_2$, and $d = 2b_2$.

[37]. In Fig. 8(b), we present the reflection coefficient under the $\mathrm{LSM}_{1,0}$ incident mode for different separation lengths between

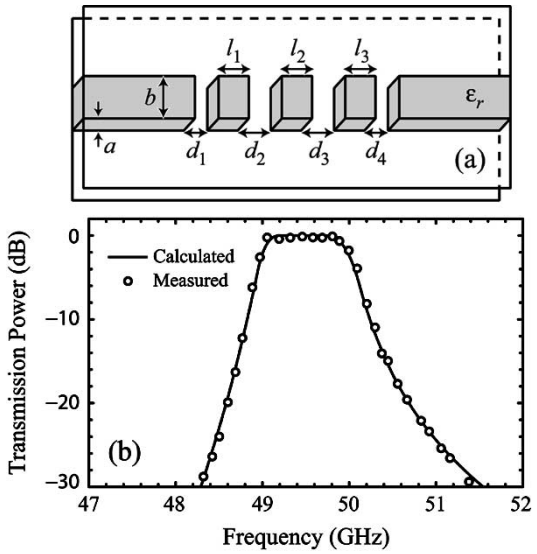


Fig. 9. Analysis of a three-pole bandpass NRD filter ($a = 2.7$ mm, $b = 3.5$ mm, $\varepsilon_r = 2.04$ (Teflon), $d_1 = d_4 = 1.6$ mm, $d_2 = d_3 = 3.5$ mm, $l_1 = l_2 = l_3 = 2.72$ mm). (a) Configuration of the filter. (b) Comparison between our theoretical results and the experimental ones presented in [27].

guides. For the case $d = 2b_2$, a dramatic reduction of the reflection coefficient over a considerable bandwidth compared to the abrupt junction $d = 0$ can be noticed, which is a consequence of the presence of the matching structure.

### C. Analysis of an NRD-Guide Filter Based on EBG Concept

Here, we are interested in the analysis of NRD-guide bandpass and stopband filters employing the EBG concept. To proceed, a versatile and accurate Fortran code has been written oriented to the rigorous analysis of complex NRD-guide circuits. To validate this software, we first compare our simulations with the experimental results presented in [27] for the three-pole bandpass filter showed in Fig. 9(a). For simulation purposes, the central cavity is formed by the three dielectric blocks (resonators) separated by the corresponding air gaps (inverters). A good agreement has been achieved in Fig. 9(b). Very good agreement is also found with other numerical results obtained in [28], fully validating our software. The CPU time requested to simulate this filter on a PC at 1000 MHz is 51 min for the numerical calculation of the first 1000 solenoidal resonant modes (the auxiliary basis is formed by 5000 modes of the empty cavity), and 1.9 s per frequency point to compute the scattering parameters.

The EBG concept in periodic dielectric structures has been widely extended for the last years for applications in both microwave and optical ranges [35], [36] in such a way that the band structure concepts of solid-state physics are applied to electromagnetic theory. Thus, infinite periodic-grating NRD-guide structures are found useful for filter design. The prediction of forbidden and allowed bands is the fundamental piece for such purposes. Following the results presented by Boone and Wu in [30], we have employed the EBG structure proposed by those authors for analyzing realistic stopband and bandpass EBG NRD-guide filters. The mentioned structure consists of an *infinite* series of dielectric stubs inserted into an NRD guide, as shown in Fig. 10(a). The period of the grating is $d + l$, where

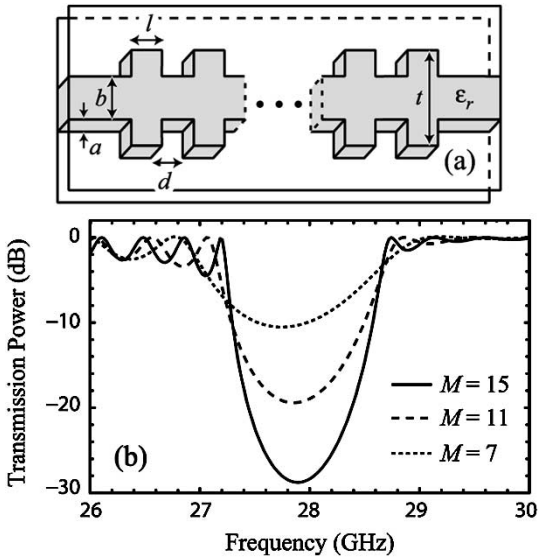


Fig. 10. Analysis of EBG NRD-guide filters ($a = 5$ mm, $b = 3.556$ mm, $\varepsilon_r = 2.56, d = l = b, t = 1.5b$). (a) Configuration of the EBG structure. (b) Transmitted power of a stopband filter under $\mathrm{LSM}_{1,0}$ incidence for a different number of periods.

$d$ is the distance between each stub and the next, and $l$ is the stub width; the stub length is denoted as $t$. In our calculations, the central resonant cavity is now formed by $M$ periods of the stub grating connected through the input and output NRD-guide ports.

The first analyzed structure is a stopband EBG NRD filter based on the forbidden bandgap predicted through the Brillouin diagram in [30, Fig. 13]. The bandgap in that figure, for the case $d = l = b$ [see Fig. 10(a)] is roughly in the frequency interval from 27.3 to 28.4 GHz. For a realistic implementation of such a filter, the number of stubs has to be *finite*. Thus, we present the EBG stopband filter in Fig. 10(a), plotting the transmittance response under an $\mathrm{LSM}_{1,0}$ excitation mode for several number of periods [see Fig. 10(b)]. As a consequence, we need to consider at least $M = 15$ periods to obtain a good filter performance enhancing the EBG behavior. The bandwidth and central frequency of this kind of filter is mainly controlled by the geometrical parameters $d, l$, and $t$. It should be noted that, in the covered frequency interval, only $\mathrm{LSM}_{1,0}$ is propagative, being evanescent the remainder of the modes. Other configurations could be provided for a specific application.

Finally, we have studied a bandpass EBG NRD-guide filter based on the concept of *localized mode at defects*, commonly used in the design of the EBG's components. For such a purpose, we have modified the width of the central stub, maintaining a constant distance between stubs. Consequently, a defect is created in the otherwise periodic structure. It is well known that defects may permit localized modes to exist with resonant frequencies inside bandgaps [35], [36]. In Fig. 11(b), we present the frequency response of the bandpass filter based on this kind of cavity for the case in which the modified width of the central stub $l' = 1.8l$. The presence of a transmission peak near 28.15 GHz can be observed, which is the only frequency in the band gap that corresponds to a cavity mode localized around the central defect. The magnetic energy density ($|\mathbf{H}(\mathbf{r})|^2$) of this resonant mode of the closed cavity is depicted in Fig. 11(a).

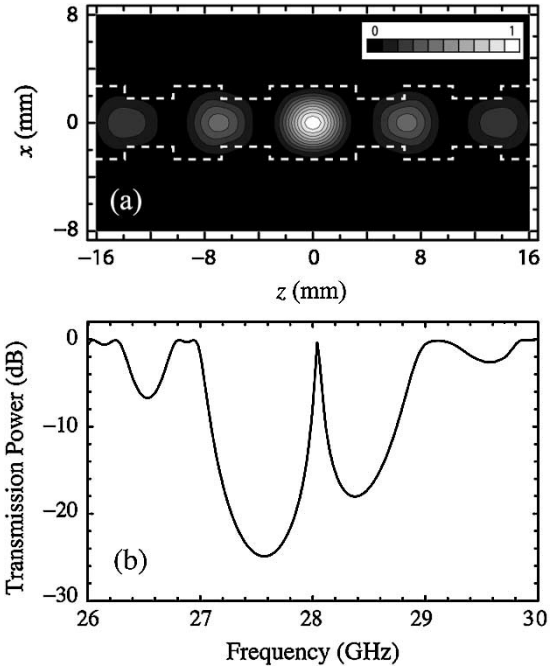


Fig. 11. (a) Normalized magnetic energy density of the resonant mode at 28.15 GHz, with $M = 15$ periods and when a defect is introduced by increasing the central stub width [see Fig. 10(a)], $l' = 1.8l$. The localized mode can be clearly visualized around the defect. (b) Transmitted power of the structure under $\mathrm{LSM}_{1,0}$ incidence showing its bandpass filter response associated to the localized mode at the central defect.

## IV. Conclusion

This paper has presented a rigorous and computationally efficient technique for modeling inhomogeneously dielectric-filled cavities connected to inhomogeneously dielectric-loaded waveguides. This method is based on the expansion of the electromagnetic field within the closed cavity in terms of their solenoidal and irrotational modes, which, in turn, have been evaluated throughout an efficient implementation of the orthonormal-basis method. The presented formulation allows the treatment of hybrid modes in the waveguide ports. Moreover, the application of the bi-orthonormal-basis method for the calculation of the full spectrum of NRD guides has been demonstrated as being a very efficient approach for the rigorous treatment of such guides. The employment of equivalent surface magnetic currents, determined by the transversal electric field at the waveguide ports, allows to efficiently compute the multimode scattering matrix of the structure. With the presented technique, we have analyzed NRD-guide components and discontinuities. In particular, we have tackled the analysis and design of a linear continuous taper to match two NRD guides with different widths, demonstrating a considerable reduction of the return losses over a wide frequency band. Finally, a stopband and bandpass NRD-guide filters based on EBG concept have been presented, proving the need for modeling realistic finite EBG devices.

## References

[1] A. Jöstingmeier, C. Rieckmann, and A. S. Omar, "Computation of the irrotational magnetic eigenfunctions belonging to complex cavities," *IEEE Trans. Microwave Theory Tech.*, vol. 42, pp. 2285–2293, Dec. 1994.

[2] V. E. Boria, S. Cogollos, H. Esteban, M. Guglielmi, and B. Gimeno, "Efficient analysis of a cubic junction of rectangular waveguides using the admittance-matrix representation," *Proc. Inst. Elect. Eng.—Microave Antennas and Propagat.*, vol. 147, pp. 417–422, Dec. 2000.
[3] S. Cogollos, V. E. Boria, H. Esteban, B. Gimeno, and M. Guglielmi, "Efficient analysis of general waveguide multi-port junctions using a segmentation technique and hybrid matrix formulations," *Ann. Telecommun.*, vol. 56, no. 1–2, pp. 94–103, 2001.
[4] M. Mattes, A. Álvarez-Melcón, M. Guglielmi, and J. R. Mosig, "Impedance representation of waveguide junctions based on the integral equation approach," in *Proc. 30th Eur. Microwave Conf.*, vol. I, Paris, France, Oct. 3–5, 2000, pp. 63–66.
[5] S. J. Fiedziuszko, I. C. Hunter, T. Itoh, Y. Kobayashi, T. Nishikawa, S. N. Stitzer, and K. Wakino, "Dielectric materials, devices, and circuits," *IEEE Trans. Microwave Theory Tech.*, vol. 50, pp. 706–720, Mar. 2002.
[6] P. Arcioni, M. Bozzi, M. Bressan, G. Conciauro, and L. Perregrini, "Frequency/time-domain modeling of 3D waveguide structures by a BI–RME approach," *Int. J. Numer. Modeling*, vol. 15, no. 1, pp. 3–21, Jan. 2002.
[7] G. Conciauro, M. Guglielmi, and R. Sorrentino, *Advanced Modal Analysis*, Chichester, U.K.: Wiley, 2000, ch. 5.
[8] M. Bressan, F. Mira, G. Conciauro, V. Boria, and B. Gimeno, "$S$-domain modeling of conducting post in rectangular waveguides by the BI–RME method," presented at the 32th Eur. Microwave Conf., Milan, Italy, Sept. 23–27, 2002.
[9] D. Kajfez, A. W. Glisson, and J. James, "Computed modal field distributions for isolated dielectric resonators," *IEEE Trans. Microwave Theory Tech.*, vol. MTT-32, pp. 1609–1616, Dec. 1984.
[10] J. Krupka, "Resonant modes in shielded cylindrical ferrite and single-crystal dielectric resonators," *IEEE Trans. Microwave Theory Tech.*, vol. 37, pp. 691–697, Apr. 1989.
[11] J. A. Pereda, L. A. Vielva, A. Vegas, and A. Prieto, "Computation of resonant frequencies and quality factors of open dielectric resonators by a combination of the finite-difference time-domain (FDTD) and Prony's methods," *IEEE Microwave Guided Wave Lett.*, vol. 2, pp. 431–433, Nov. 1992.
[12] N. Kaneda, B. Houshmand, and T. Itoh, "FDTD analysis of dielectric resonators with curved surfaces," *IEEE Trans. Microwave Theory Tech.*, vol. 45, pp. 1645–1649, Sept. 1997.
[13] D. Kremer and R. Pregla, "The method of lines for the hybrid analysis of multilayered cylindrical resonator structures," *IEEE Trans. Microwave Theory Tech.*, vol. 45, pp. 2152–2155, Dec. 1997.
[14] C. Wang and K. A. Zaki, "Generalized multilayer anisotropic dielectric resonators," *IEEE Trans. Microwave Theory Tech.*, vol. 48, pp. 60–66, Jan. 2000.
[15] W. Yu and R. Mittra, "A conformal finite difference time domain technique for modeling curved dielectric surfaces," *IEEE Microwave Wireless Comp. Lett.*, vol. 11, pp. 25–27, Jan. 2001.
[16] Y. M. Poplavko, Y. V. Prokopenko, V. I. Molchanov, and A. Dogan, "Frequency-tunable microwave dielectric resonator," *IEEE Trans. Microwave Theory Tech.*, vol. 49, pp. 1020–1026, June 2001.
[17] J. A. Monsoriu, M. V. Andrés, E. Silvestre, A. Ferrando, and B. Gimeno, "Analysis of dielectric-loaded cavities using an orthonormal-basis method," *IEEE Trans. Microwave Theory Tech.*, vol. 50, pp. 2545–2552, Nov. 2002.
[18] A. Jöstingmeier and A. S. Omar, "Analysis of inhomogenously filled cavities coupled to waveguides using the VIE formulation," *IEEE Trans. Microwave Theory Tech.*, vol. 41, pp. 1207–1214, June/July 1993.
[19] H. Esteban, S. Cogollos, V. E. Boria, A. S. Blas, and M. Ferrando, "A new hybrid mode-matching/numerical method for the analysis of arbitrarily shaped inductive obstacles and discontinuities in rectangular waveguides," *IEEE Trans. Microwave Theory Tech.*, vol. 50, pp. 1219–1224, Apr. 2002.
[20] D. Baillargeat, S. Verdeyme, M. Aubourg, and P. Guillon, "CAD applying the finite-element method for dielectric-resonator filters," *IEEE Trans. Microwave Theory Tech.*, vol. 46, pp. 10–17, Jan. 1998.
[21] G. Macchiarella, M. Fumagalli, and S. C. d'Oro, "A new coupling structure for dual mode dielectric resonators," *IEEE Microwave Guided Wave Lett.*, vol. 10, pp. 523–525, Dec. 2000.
[22] A. R. Weily and A. S. Mohan, "Microwave filters with improved spurious performance based on sandwiched conductor dielectric resonators," *IEEE Trans. Microwave Theory Tech.*, vol. 49, pp. 1501–1507, Aug. 2001.
[23] K. Kurokawa, *An Introduction to the Theory of Microwave Circuits*. New York: Academic, 1969.
[24] R. E. Collin, *Field Theory of Guided Waves*, 2nd ed. New York, NY: IEEE Press, 1991.
[25] P. Przybyszewski, J. Mielewski, and M. Mrozowski, "A fast technique for analysis of waveguides," *IEEE Microwave Guided Wave Lett.*, vol. 8, pp. 109–111, Mar. 1998.
[26] T. Yoneyama and S. Nishida, "Nonradiative dielectric waveguide for millimeter wave integrated circuits," *IEEE Trans. Microwave Theory Tech.*, vol. MTT-29, pp. 1188–1192, Nov. 1981.
[27] T. Yoneyama, F. Kuroki, and S. Nishida, "Design of nonradiative dielectric waveguide filters," *IEEE Trans. Microwave Theory Tech.*, vol. MTT-32, pp. 1659–1662, Dec. 1984.
[28] S. Xu, X. Wu, and T. Yoneyama, "Scattering properties of dicontinuities in NRD guide," *Proc. Inst. Elect. Eng.—Microave Antennas and Propagat.*, vol. 141, no. 3, pp. 205–210, June 1994.
[29] J. Dallaire and K. Wu, "Complete characterization of transmission losses in generalized nonradiative dielectric (NRD) waveguide," *IEEE Trans. Microwave Theory Tech.*, vol. 48, pp. 121–125, Jan. 2000.
[30] F. Boone and K. Wu, "Mode conversion and design consideration of integrated nonradiative dielectric (NRD) components and discontinuities," *IEEE Trans. Microwave Theory Tech.*, vol. 48, pp. 482–492, Apr. 2000.
[31] E. Silvestre, M. V. Andres, and P. Andrés, "Biorthonormal-basis method for the vector description of optical-fiber modes," *J. Lightwave Technol.*, vol. 16, pp. 923–928, May 1998.
[32] E. Silvestre, M. A. Abian, B. Gimeno, A. Ferrando, M. V. Andrés, and V. E. Boria, "Analysis of inhomogeneously filled waveguides using a bi-orthonormal-basis method," *IEEE Trans. Microwave Theory Tech.*, vol. 48, pp. 589–596, Apr. 2000.
[33] J. Van Bladel, *Electromagnetic Fields*. Washington, DC: Hemisphere, 1985.
[34] J. A. Monsoriu, A. Coves, B. Gimeno, M. V. Andrés, and E. Silvestre, "A robust and efficient method for obtaining the complex modes in inhomogeneously filled waveguides," *Microwave Opt. Technol. Lett.*, vol. 37, no. 3, pp. 218–222, May 2003.
[35] J. D. Joannopoulos, R. D. Meade, and J. N. Winn, *Photonic Crystals: Molding the Flow of Light*. Princeton, NJ: Princeton Univ. Press, 1995.
[36] A. L. Reynolds, U. Peschel, F. Lederer, P. J. Roberts, T. F. Krauss, and P. J. I. de Maagt, "Coupled defects in photonic crystals," *IEEE Trans. Microwave Theory Tech.*, vol. 49, pp. 1860–1867, Oct. 2001.
[37] S. J. Xu, X.-Y. Zeng, K. Wu, and K.-M. Luk, "Characteristics and design consideration of leaky-wave NRD-guides for use as millimeter-wave antenna," *IEEE Trans. Microwave Theory Tech.*, vol. 46, pp. 2450–2456, Dec. 1998.

**Juan A. Monsoriu** was born in Valencia, Spain, in 1975. He received the Licenciado, M.S., and Ph.D. degrees in physics from the Universidad de Valencia, Valencia, Spain, in 1998, 2000, and 2003, respectively.

Since 2000, he has been an Assistant Professor with the Departamento de Física Aplicada, Universidad Politécnica de Valencia, Valencia, Spain. His main research interests are modal methods for the design of inhomogeneous waveguides, dielectric resonators, and microstructured opto-electronic devices.

**Benito Gimeno** (M'01) was born in Valencia, Spain, on January 29, 1964. He received the Licenciado degree in physics and Ph.D. degree from the Universidad de Valencia, Valencia, Spain, in 1987 and 1992, respectively.

From 1987 to 1990, he was a Fellow with the Universidad de Valencia. Since 1990, he has been an Assistant Professor with the Departmento de Física Aplicada, Universidad de Valencia, where he became Associate Professor in 1997. From 1994 to 1995, he was a Research Fellow with the European Space Research and Technology Centre (ESTEC), European Space Agency (ESA). In 2003, he spent three months as a Visiting Scientist with the Universita degli Studi di Pavia, Pavia, Italy. His current research interests include the areas of computer-aided techniques for analysis of microwave passive components, waveguide and cavities structures including dielectric resonators, and photonic bandgap crystals.

**Enrique Silvestre** was born in Valencia, Spain, in 1962. He received the Licenciado degree in physics, M.Sc. degree in theoretical physics, M.Sc. degree in optics, and Ph.D. degree in physics from the Universidad de Valencia, Valencia, Spain, in 1986, 1989, 1997, and 1999, respectively.

In 1997, he was an Assistant Professor with the Departamento de Óptica, UV. From 1999 to 2000, he was with the Department of Physics, University of Bath, Bath, U.K., where he was a Research Officer. Since 2001, he has been an Associate Professor with the Universidad de Valencia. His research interests are modal techniques for electromagnetic-wave propagation in nonsymmetrical structures and photonic crystals.

**Miguel V. Andrés** (M'91) was born in Valencia, Spain, in 1957. He received the Licenciado en Física degree and Doctor en Física (Ph.D.) degree from the Universidad de Valencia, Valencia, Spain, in 1979 and 1985, respectively.

Since 1983, he has served successively as an Assistant Professor and Lecturer with the Departamento de Física Aplicada, Universidad de Valencia. From 1984 to 1987, he was with the Department of Physics, University of Surrey, U.K., as a Visiting Research Fellow. Until 1984, he was engaged in research on microwave surface waveguides. His current research interests include waveguide theory (inhomogeneous waveguides and microstructured optical fibers) and optical fiber devices and systems for microwave photonics and sensor applications (optical fiber interferometers, evanescent field devices based on optical fiber tapers, in-fiber Bragg gratings, and photonic crystal fibers).

Dr. Andrés is a member of the Optical Society of America (OSA) and the Institute of Physics (IOP).